



# Numerical study of turbulent flow with heat removal from a flat plate using the finite volume-based method of lines

Numerical study of turbulent flow

511

Antonio Campo  
 College of Engineering, Idaho State University, Pocatello,  
 Idaho, USA

Received October 2000

Revised April 2001

Accepted April 2001

**Keywords** Thermodynamics, Modelling

**Abstract** A hybrid computational method has been developed for the calculation of momentum and heat transfer in turbulent boundary layer flows along flat plates. The proposed method, the finite volume-based method of lines, replaces a partial differential equation and two independent variables by a system of ordinary differential equations of first order and one independent variable. Using the simplest assumptions for modeling the turbulent diffusivity of momentum and heat, the system of differential equations may be readily integrated with a fourth-order Runge-Kutta algorithm. To validate the numerical predictions, comparisons with experimental data for air have been done in terms of axial velocities, temperatures, skin friction coefficients and Stanton numbers. For the wide range of Reynolds numbers tested, the hydrodynamic and thermal characteristics of turbulent air flows are predicted correctly.

## Nomenclature

$A^+$  = van Driest constant  
 $C$  = specific heat capacity  
 $C_f$  = local skin friction coefficient  
 $K$  = constant, equation (11)  
 $l$  = mixing length  
 $Pr$  = Prandtl number  
 $Pr_t$  = turbulent Prandtl number  
 $q_w$  = wall heat flux  
 $Re_x$  = local Reynolds number  
 $Re_\theta$  = momentum thickness Reynolds number  
 $St$  = Stanton number  
 $S_\phi$  = source term, equation (8)  
 $t$  = temperature  
 $t_w$  = wall temperature  
 $t_\infty$  = free stream temperature  
 $t^+$  = non-dimensional temperature,  
 $\frac{(t_w - t)(\tau_w / \rho)^{1/2}}{q_w / \rho c}$   
 $u$  = axial velocity component  
 $u^+$  = non-dimensional axial velocity,  $u/u_\tau$   
 $u_\tau$  = shear velocity,  $(\tau_w / \rho)^{1/2}$   
 $u_\infty$  = free stream velocity  
 $v$  = transversal velocity component  
 $x$  = axial coordinate

$y$  = transversal coordinate  
 $y^+$  = non-dimensional transversal coordinate,  $\frac{y u_\tau}{\nu}$

## Greek letters

$\alpha$  = molecular thermal diffusivity  
 $\Gamma_{eff}$  = effective diffusion coefficient, equation (8)  
 $\Delta y$  = transversal interval  
 $\delta$  = thickness of the boundary layer  
 $\epsilon_H$  = eddy diffusivity for heat  
 $\epsilon_M$  = eddy diffusivity for momentum  
 $\nu$  = kinematic viscosity  
 $\rho$  = density  
 $\tau_w$  = wall shear stress  
 $\phi$  = generalized transport variable, equation (8)

## Subscripts

$i$  = inner  
 $n$  = north line  
 $o$  = outer  
 $p$  = line  
 $s$  = south line

**Introduction**

The art of predicting the hydrodynamic and thermal turbulent boundary layers in external flows has advanced very rapidly with the development of sophisticated finite-difference procedures and the advent of large-scale digital computers. The complexity inherent in the calculation of boundary layers has motivated researchers to improve existing numerical procedures until accurate numerical predictions of the experimental data, coupled with small computing costs could be met. Typical studies can be found in Pletcher (1969), Patankar and Spalding (1970), Cebeci *et al.* (1970), Dyban and Fridman (1987), Zincheno and Fedorova (1987), Shishov (1991), Susec and Oljaca (1995), Hori and Yata (1997), Volino and Simon (1997) and Silva Freire (1999). In these works, quite satisfactory numerical results have been obtained for both skin friction and heat transfer coefficients in turbulent boundary layers of incompressible fluids. Standard finite-difference techniques demand that the streamwise and transversal intervals of the governing conservation equations must be chosen sufficiently small to force the numerical solution to converge closely to the exact solution.

From a conceptual point of view, the lack of a complete statistical theory for the turbulent transport of mass, momentum and energy has been the main obstacle for the exact determination of time-mean velocity and time-mean temperature fields (Schlichting, 1979). Therefore, the solutions of the conservation equations of the turbulent boundary layers depend on some empiricism based on experimental data. Consequently, this situation has led to the adoption of various approaches and methodologies that provide a wide spectrum of accuracy in predicting the relevant boundary layer parameters.

The general objective of this investigation was to develop a simple and reliable computational procedure of explicit type for the calculation of the hydrodynamic and thermal boundary layers along flat plates. Based on its flexible characteristics, the procedure is intended to be suitable for both research and educational purposes in engineering. The path followed here is briefly outlined below:

- (1) A numerical methodology involving the method of lines (MOL) (Liskovets, 1965) has been implemented and modified for the treatment of the conservation equations of mass, momentum and energy. A variant of the method, the finite volume method of lines (FVMOL) is introduced wherein the discretization of the transversal derivatives in the conservation equations was performed with finite volumes (Tannehill *et al.*, 1997). The finite volumes have to be constructed in a special way such that their sizes have infinitesimal length and finite height. Accordingly, the original set of conservation equations is reformulated by a system of ordinary differential equations of first order where the streamwise coordinate retaining a continuous behavior is the independent variable. In turn, the resulting initial value problem (IVP) may be readily integrated numerically with a fourth-order Runge-Kutta algorithm.

- (2) In the above formulation, the hydrodynamic boundary layer is envisioned as a composite layer having two regions: an inner and an outer region. The most simple continuous model for the eddy diffusivity of momentum was utilized, i.e. the mixing length model. Additionally, the eddy diffusivity of heat was expressed in terms of a turbulent Prandtl number, which was assumed to be constant.
- (3) The experimental data most heavily relied on were expressed in terms of global quantities, such as the skin friction coefficient and the Stanton number for air flows characterized by Reynolds numbers ranging from  $10^5$  to  $10^7$ . In addition, comparisons were also made with experimental measurements of local quantities: the non-dimensional axial velocity  $u$  and the non-dimensional temperature  $t$ .

FVMOL may handle equally well turbulent flows exposed to large temperature differences. The properties appearing in the equations of conservation have to be taken as variables, so that the equations are highly coupled. Needless to say, more refined models for the eddy diffusivity of momentum and the eddy diffusivity of heat may be incorporated into the conservation equations too, without causing additional difficulties.

### Descriptive equations

Under the assumption of constant properties, the time-averaged conservation equations of mass, momentum and energy for a turbulent boundary layer flow along a flat plate are:

Mass:

$$\frac{\partial u}{\partial x} + \frac{\partial v}{\partial y} = 0, \quad (1)$$

Momentum:

$$u \frac{\partial u}{\partial x} + v \frac{\partial u}{\partial y} = \frac{\partial}{\partial y} \left[ (\nu + \varepsilon_M) \frac{\partial u}{\partial y} \right], \quad (2)$$

Energy:

$$u \frac{\partial t}{\partial x} + v \frac{\partial t}{\partial y} = \frac{\partial}{\partial y} \left[ (\alpha + \varepsilon_H) \frac{\partial t}{\partial y} \right]. \quad (3)$$

The incoming fluid has a uniform free-stream velocity  $u_\infty$  and a uniform free-stream temperature  $t_\infty$ , while the plate is maintained at a uniform temperature,  $t_w$ .

#### *Zero-equation model*

For the closure of the turbulence, the simplest algebraic turbulence model is the mixing length model of Prandtl (Schlichting, 1979). Accordingly, the eddy diffusivity for momentum  $\varepsilon_M$  is:

$$\varepsilon_M = l^2 \left| \frac{\partial u}{\partial y} \right|, \quad (4)$$

where  $l$  denotes the “mixing length”. To account for the inner region, the variable “mixing length” is evaluated with:

**514**

---


$$l_i = \kappa y \left[ 1 - \exp\left(-\frac{y^+}{A^+}\right) \right], \quad (5)$$

where  $y^+ = (yu_\tau/\nu)$  is the wall coordinate,  $\kappa = 0.4$  is the von Kármán constant and  $A^+ = 25$  is the damping constant (van Driest, 1956). The outer region is modeled by a constant “mixing length”:

$$l_o = C \delta, \quad (6)$$

where  $C = 0.089$  and  $\delta$  is the hydrodynamic boundary layer thickness. This relation was derived by Maise and McDonald (1968) and agrees well with the experimental data. Consequently, equation (5) applies from the wall up to a certain location wherein  $l_i = l_o$ , and beyond this merging point equation (6) is utilized.

At this point, it is worth mentioning that the computational methodology to be described in the next section has no intrinsic limitations that would prevent the utilization of more refined algebraic turbulence models.

The turbulent diffusivity for heat  $\varepsilon_H$  may be expressed by:

$$\varepsilon_H = \frac{\varepsilon_M}{Pr_t}, \quad (7)$$

where the turbulent Prandtl number  $Pr_t$  for air takes as a constant value equal to 0.85 (Kays, 1994). Again, it is appropriate to reiterate that more elaborate models for  $Pr_t$  may be incorporated in the analysis. However, as mentioned before, the primary aim of this paper was to resort to the simplest models.

### Computational methodology

It is important to recognize that although turbulence models may be carefully formulated, sometimes predictions cannot be improved beyond a certain level because of the inherent limitations of the finite-difference method adopted. Various schemes have been extensively used in computational fluid dynamics because of their simplicity and good stability characteristics when applied to external turbulent flows (Tannehill *et al.*, 1997). Obviously, the merits of a higher-order closure turbulence model can be easily lost in the computational process.

#### *Background*

In general, two-dimensional boundary layer flows require the solution of a system of three partial differential equations. Each equation in the system may be accommodated into a generalized convection-diffusion transport equation:

$$\frac{\partial}{\partial x}(u\phi) + \frac{\partial}{\partial y}(v\phi) = \frac{\partial}{\partial y}\left(\Gamma_{\text{eff}} \frac{\partial \phi}{\partial y}\right) + S_{\phi}, \quad (8)$$

where  $\phi$  represents a generic transport variable,  $\Gamma_{\text{eff}}$  is the effective diffusion coefficient and  $S_{\phi}$  is the source term, respectively (see Table I).

Any standard finite-difference method approximates equation (8) at any interior point  $i,j$  of the computational domain by an algebraic equation accounting for a five-point molecule. Thus, having such an algebraic equation for each interior point, the main task is to solve a system of algebraic equations for the unknown quantities  $\phi$ .

*The new proposed method: FVMOL*

From a mathematical perspective, the MOL is essentially a hybrid technique for replacing a partial differential equation in two independent variables by an appropriate system of ordinary differential equations in one variable (Liskovets, 1965). If the partial differential equation is parabolic, having independent variables  $x$  (axial variable) and  $y$  (transversal variable), as in equation (8), then the region of integration may be divided into lines parallel to the  $x$ -coordinate by lines  $y = \text{constant}$ . Thus, the partial derivatives of  $\phi$  with respect to  $y$  at each line are replaced by standard finite-difference formulations using values of the dependent variables at a particular line and at the upper and lower adjacent lines. This systematic procedure gives rise to a system of ordinary differential equations of first order, where the dependent variable  $\phi$  along each line depends solely on the continuous independent variable,  $x$ .

Instead of standard finite-difference formulations, the discretization procedure in this work relies on finite volumes (Tannehill *et al.*, 1997). This combination generates a hybrid method called the FVMOL, wherein the finite volume shown in Figure 1 has infinitesimal length in the axial direction and finite height in the transverse direction. Actually, this study represents another step in the development of simple computational methodologies for partial differential equations involving discretizations by finite volumes.

The region of integration is divided into an array of lines parallel to the wall as illustrated in Figure 2. Correspondingly, equation (8) may be integrated in the  $y$ -direction between the appropriate limits of integration  $s$  and  $n$ . This integration gives the following equation:

Conservation equations	$\phi$	$\Gamma_{\text{eff}}$	$S_{\phi}$
Mass	1	0	0
Momentum	u	$\nu + \epsilon_M$	0
Energy	t	$\alpha + \epsilon_H$	0

**Table I.**  
Variables in  
equation (8)

**Figure 1.**  
One-dimensional finite  
volume

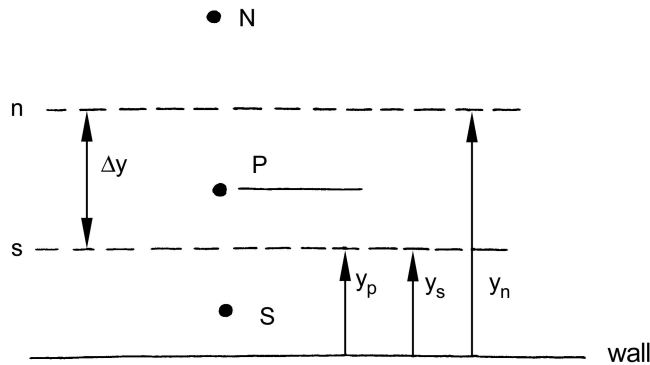
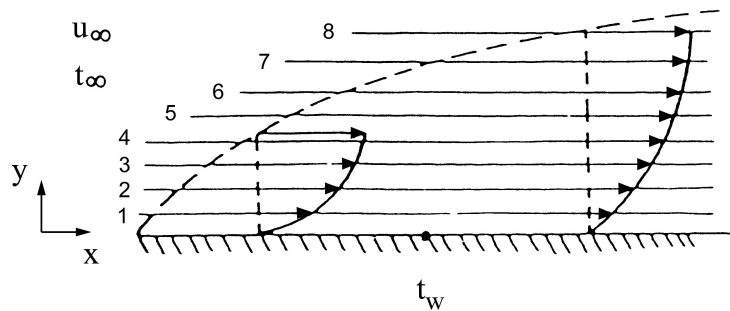


**Figure 2.**  
Distribution of lines in the  
computational  
domain



$$\int_s^n \frac{\partial}{\partial x} (u\phi) dy + (v\phi)_n - (v\phi)_s = \left( \Gamma_{\text{eff}} \frac{\partial \phi}{\partial y} \right)_n - \left( \Gamma_{\text{eff}} \frac{\partial \phi}{\partial y} \right)_s + \int_s^n S_\phi dy, \quad (9)$$

which is “exact” in the sense that no additional hypothesis has been invoked so far. Next, assuming that the field variables  $u$ ,  $v$ ,  $\phi$ , as well as  $S_\phi$  may be considered nearly constant between the boundaries  $s$  and  $n$  of the finite volume, equation (9) is converted into the ordinary differential equation of first order:

$$\frac{d}{dx} (u_p \phi_p) = \frac{1}{\Delta y} \left( \Gamma_{\text{eff}} \frac{\partial \phi}{\partial y} - v\phi \right)_s + S_{\phi p}. \quad (10)$$

Thus, from a mathematical point of view, equation (10) governs the continuous variation of each field variable in the  $x$  direction at any fixed distance,  $y = y_p$ , measured from the wall.

The diffusive term appearing at the upper and lower faces of the finite volume is taken into account by utilizing an appropriate logarithmic law for the variation of each field variable between neighboring lines. To do so, a logarithmic law has been adopted because both the axial velocity and the

temperature profiles usually exhibit smooth and almost linear variation with the logarithm of the transversal space variable  $y$ .

*Non-uniform transversal intervals*

Adoption of a non-uniform grid in the  $y$ -direction may be beneficial because it reduces the number of lines in the computational domain, and consequently reduces the number of ordinary differential equations of first order that participate in the system. This particular grid produces smaller intervals close to the wall and larger intervals near the edge of the boundary layer. As a result, the grid accommodates larger axial velocity and temperature gradients in the vicinity of the wall. Correspondingly, the deployment of lines responds to the relation:

$$\ln \frac{y_u}{y_d} = K, \tag{11}$$

which has the property that the logarithm of the ratio of distances from the wall to any two adjacent lines is a constant value  $K$  (see Figure 3). Moreover, it is also assumed that the common boundary,  $c$ , between two consecutive lines,  $u$  and  $d$ , lies at a distance  $y$  from the wall, satisfying the relation:

$$\frac{\ln (y_c/y_d)}{\ln (y_u/y_d)} = \frac{1}{2}. \tag{12}$$

Also, it may be assumed that there exists a logarithmic profile for any field variable  $\phi$  (axial velocity  $u$  and temperature  $t$ ) between two consecutive lines,  $u$  and  $d$ , of the form:

$$\phi = a \ln (by). \tag{13}$$

As a consequence of these steps, the diffusivity flux of  $\phi$  across the boundary  $c$  becomes:

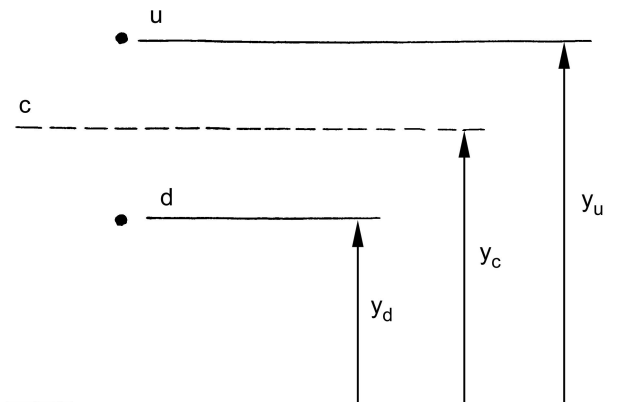


**Figure 3.**  
Variable  
transversal grid

$$\Gamma_c \left( \frac{\partial \phi}{\partial y} \right)_c = \Gamma_c \left( \frac{\phi_u - \phi_d}{Ky_c} \right), \quad (14)$$

once the constants a and b have been computed.

### Transformation of the descriptive equations

Equation (10), with information from Table I, supplies the system of  $y$ -discretized equations that describe the conservation of mass, momentum and energy:

Momentum:

$$\frac{du_p}{dx} = \frac{1}{\Delta y(2u_p - u_n)} \left\{ \left[ (\nu + \varepsilon_M) \frac{\partial u}{\partial y} \right]_s^n - v_s(u_s - u_n) \right\}, \quad (15)$$

Mass:

$$v_n = v_s - \Delta y \frac{du_p}{dx}, \quad (16)$$

Energy:

$$\frac{dt_p}{dx} = \frac{1}{u_p \Delta y} \left[ \Lambda_m - vt \right]_s^n - \frac{t_p}{u_p} \frac{du_p}{dx}, \quad (17)$$

where:

$$\Lambda_M = \frac{\alpha}{\nu} + \frac{\varepsilon_H}{\nu} = \frac{1}{Pr} + \frac{\varepsilon_M/\nu}{Pr_t}, \quad (18)$$

is an auxiliary function.

The system of equations (15)-(18) describes an IVP where the boundary conditions at the leading edge of the plate are:

$$u_p = u_\infty, \quad t_p = t_\infty, \quad x = 0. \quad (19)$$

### Computational procedure

The above system of equations implies that the axial velocity  $u$ , the transversal velocity  $v$  and the temperature  $t$  may be explicitly calculated inside the hydrodynamic and thermal boundary layers moving from the wall outwards. In the vicinity of the wall, the axial velocity has been modeled by postulating the existence of a Couette flow, which allows for the diffusive momentum interchange between lines W and P in Figure 4 (Tannehill *et al.*, 1997). As a result, the finite volume formulation in the transversal direction avoids the regions of large gradients close to the wall.

Starting with three lines at the leading edge of the plate, the number of lines that need to be placed inside the turbulent boundary layer may be determined at each axial step (see Figure 2). As a by-product, the gradually increasing



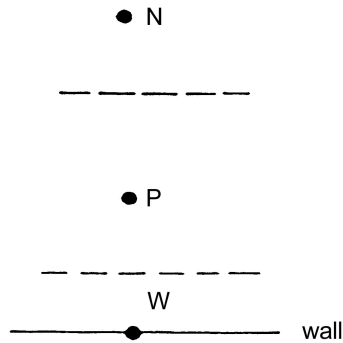


**Figure 4.**  
One-dimensional finite  
volume near the wall

number of lines serves to delineate the natural growth of the turbulent boundary layers such that the condition at the outer edge  $u/u_\infty > 0.99$ . The system of equations (15)-(19) was numerically integrated with a fourth-order Runge-Kutta algorithm (IMSL, 1984) on a personal computer. A sensitivity analysis of the grid produced grid-independent results for 16 unequally spaced intervals at the trailing edge of the plate and an axial step of  $10^{-4}$ .

### Calculated and experimental results

The numerical calculations were performed for turbulent air flows in the range  $10^5 < Re_x < 10^7$  and  $Pr = 0.7$ .

A typical distribution of wall velocity is plotted on wall coordinates in Figure 5. Good agreement is observed with the experimental observations of Anderson *et al.* (1975) for the various Reynolds number  $Re_x$  tested at both the

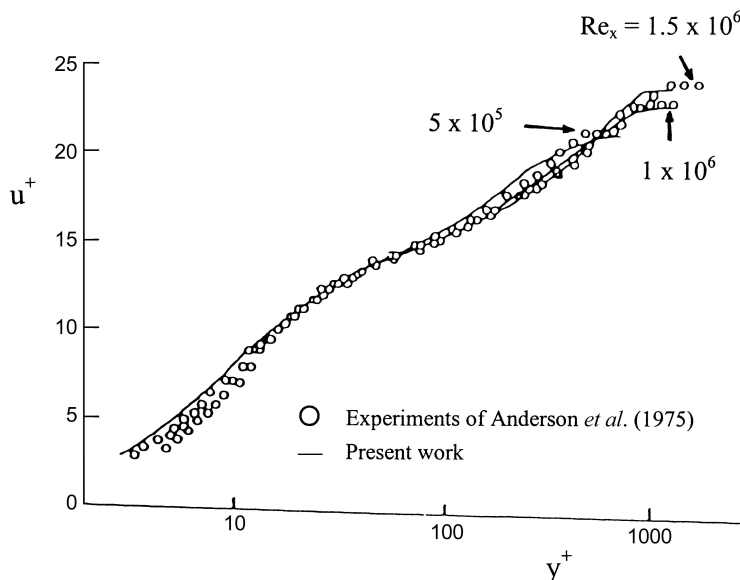


**Figure 5.**  
Turbulent velocity  
profile

inner and outer regions of the turbulent boundary layer of air ( $1 < y^+ < 1,000$ ). Similarly, the predicted velocity profiles are also in agreement with the logarithmic portion of the law of the wall.

Figure 6 compares the experimental and numerical results for the variation of the skin friction coefficient  $C_f$  (a global quantity) with the momentum thickness Reynolds number  $Re_\theta$ . An overall inspection of part a in the figure reveals that good agreement prevails between the majority of experimental data points for air and the numerical results for the interval  $4 \times 10^2 < Re_\theta < 10^4$ . The same set of  $C_f$  results is plotted in part b of the figure, along with those of Pletcher (1969) calculated by an explicit finite-difference method. It may be confirmed that both curves overlap over the  $Re_\theta$  interval employed. Furthermore, the monotonic decreasing curve compares well with the standard correlation equation given by Schlichting (1979):

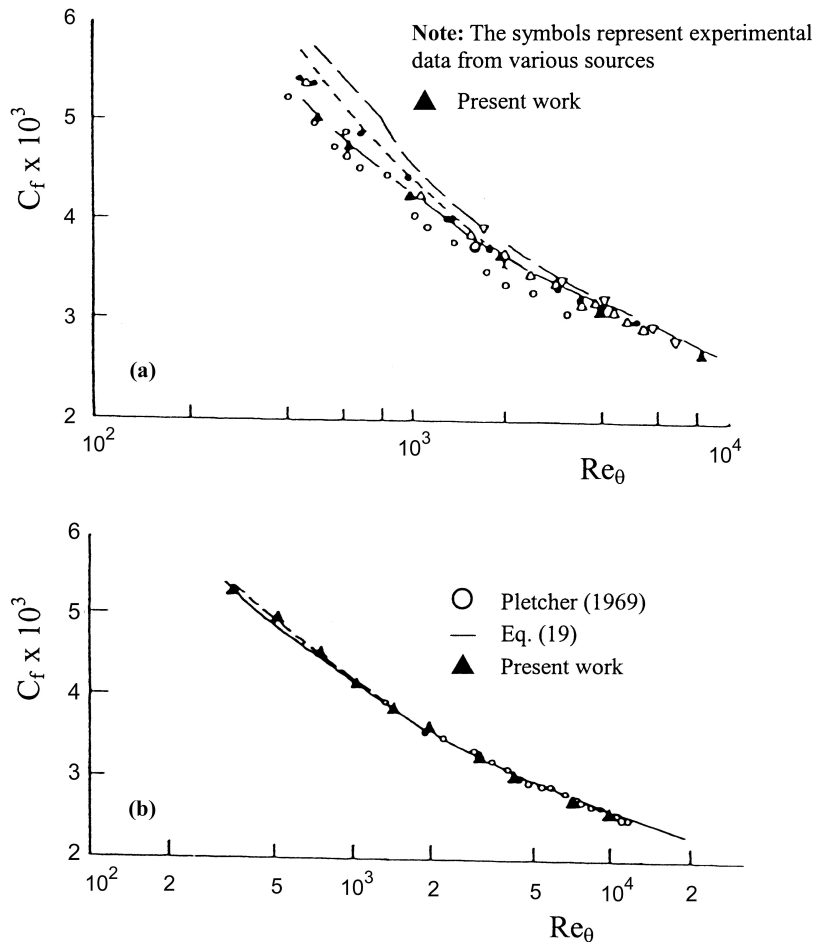


**Figure 6.**  
Skin friction coefficient  
vs. Reynolds number

$$C_f = 0.0256 \text{Re}_\theta^{-1/4}. \quad (20)$$

Attention is now directed to the heat transfer between the wall and air ( $\text{Pr} = 0.7$ ). These results include temperature distributions and local Stanton numbers for  $\text{Re}_x = 1.2 \times 10^6$ . The non-dimensional temperature distribution designated as  $t^+$  vs  $y^+$  will be discussed first. In Figure 7, it is observed that the numerical predictions exhibit a good qualitative trend when compared with the measurements of Blackwell (1972). Moreover, the Stanton number  $St$  is plotted as a function of the Reynolds number  $\text{Re}_x$  in Figure 8. This figure confirms the expected monotonic decrease of the turbulent convective heat transfer coefficient of the air flow along the plate. It may be seen that there is no appreciable deviation between the numerical estimation and the experimental measurements reported by Reynolds *et al.* (1958) over the range  $2 \times 10^5 < \text{Re}_x < 8 \times 10^6$ . It is common practice to identify this variation by a simple correlation equation proposed by Reynolds *et al.* (1958):

$$St \text{Pr}^{0.4} = 0.0287 \text{Re}_x^{-0.2}. \quad (21)$$

### Concluding remarks

This paper presented a numerical simulation of the hydrodynamic and thermal characteristics of turbulent flows along an isothermal flat plate. The numerical portion of the work was based on a suitable combination of the FVMOL. On discretizing the transversal derivatives of the conservations equations of mass, momentum and energy, a system of first-order ordinary differential equations

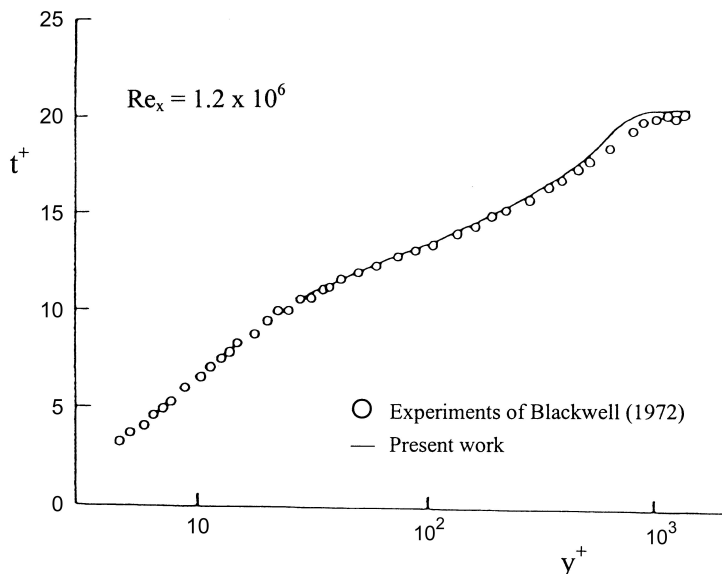
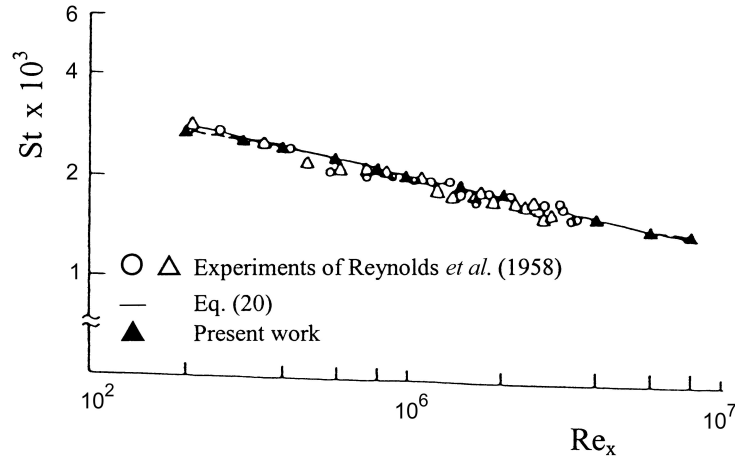


**Figure 7.**  
Turbulent temperature  
profile

**Figure 8.**  
Stanton number vs  
momentum thickness  
Reynolds number



is readily obtained. This system may be easily solved by a marching technique, such as the fourth order Runge-Kutta yielding the distributions of axial velocity, transverse velocity and temperature. Excellent agreement was found to prevail between the numerical predictions and the experimental data for air for the global quantities, such as the skin friction coefficients and the Stanton numbers utilizing three lines at the leading edge and a maximum of 16 lines at the trailing edge. The excellence of these agreements gives confidence in the capabilities of the hybrid numerical procedure (FVMOL) to produce results of high accuracy for the hydrodynamic and thermal developments of boundary layers of common liquids under turbulent conditions.

### References

- Anderson, P.S., Kays, W.M. and Moffat, R.J. (1975), "Experimental results for the transpired boundary layer in an adverse pressure gradient", *J. Fluid Mechanics*, Vol. 69, pp. 353-75.
- Blackwell, B.F. (1972), PhD thesis, Stanford University, Stanford, CA.
- Cebeci, T., Smith, A. and Mosinskis, G. (1970), "Solution of the incompressible turbulent boundary layer equations with heat transfer", *J. Heat Transfer*, Vol. 90, pp. 133-43.
- Dyban, E.P. and Fridman, E.A. (1987), "A numerical simulation of the thermal boundary layer of turbulent flow over a plate", *Promyshlennaya Teplotekhnika*, Vol. 9 No. 6.
- Hori, M. and Yata, J. (1997), "Effects of free stream turbulence on turbulent boundary layer on a flat plate with zero pressure gradient" (Part V: The calculation of heat transfer), *Heat Transfer-Japanese Research*, Vol. 26 No. 2.
- IMSL (1984), *Library Subroutine Package*, IMSL Inc., Houston, TX.
- Kays, W.M. (1994), "Turbulent Prandtl number – where are we?", *Journal of Heat Transfer*, Vol. 116, pp. 284-95.
- Liskovets, O.A. (1965), "The method of lines" (Review), *Differential Equations*, Vol. 1, pp. 1308-23.
- Maise, G. and McDonald, H. (1968), "Mixing length and kinematic eddy viscosity in a compressible boundary layer", *AIAA J*, Vol. 6, pp. 73-80.
- Patankar, S.V. and Spalding, D.B. (1970), *Heat and Mass Transfer in Boundary Layers*, 2nd ed., Intertext, London.

- 
- Pletcher, R.H. (1969), "On a finite-difference solution for the constant property turbulent boundary layer", *AIAA J*, Vol. 7, pp. 305-11.
- Reynolds, W.C., Kays, W.M. and Kline, S.J. (1958), "Heat transfer in the turbulent incompressible boundary layer I: constant wall temperature", *NASA Memo*, 12-2-58W.
- Schlichting, H. (1979), *Boundary Layer Theory*, McGraw-Hill, New York, NY.
- Shishov, E.V. (1991), "Turbulent heat and momentum transfer in boundary layers under strong pressure gradient conditions: analysis of experimental data and numerical prediction", *Experimental Thermal and Fluid Sciences*, Vol. 4 No. 4.
- Silva Freire, A.P. (1999), "On Kaplun limits and the multilayered asymptotic structure of the turbulent boundary layer", *Hybrid Methods in Engineering*, Vol. 1 No. 3.
- Susec, J. and Oljaca, M. (1995), "Calculation of turbulent boundary layers with transpiration and pressure gradient effects", *International Journal of Heat Mass Transfer*, Vol. 38 No. 15.
- Tannehill, J.C., Anderson, D.A. and Pletcher, R.H. (1997), *Computational Fluid Mechanics and Heat Transfer*, 2nd ed., Taylor and Francis, Washington, DC.
- Van Driest, E.R. (1956), "On turbulent flow near a wall", *J. Aeronautical Sciences*, Vol. 23, pp. 1007-10.
- Volino, R.J. and Simon, T.W. (1997), "Velocity and temperature profiles in turbulent boundary layer flows experiencing streamwise pressure gradients", *Journal of Heat Transfer*, Vol. 119 No. 3.
- Zincheno, V.I. and Fedorova, O.P. (1987), "Combined heat transfer in a spatial turbulent boundary layer", *Zhurnal Prikladnoi Mekhaniki I Tekhnicheskoi Fiziki*, No. 3.